NASA TECHNICAL MEMORANDUM

NASA TM X-52270

NASA TM X- 52270

A METHOD OF ESTIMATING HIGH TEMPERATURE LOW CYCLE FATIGUE BEHAVIOR OF MATERIALS

by S. S. Manson and Gary Halford
Lewis Research Center
Cleveland, Ohio

NATIONAL AERONAUTICS AND SPACE ADMINISTRATION · WASHINGTON, D.C. · 1967

A METHOD OF ESTIMATING HIGH TEMPERATURE LOW CYCLE

FATIGUE BEHAVIOR OF MATERIALS

by S. S. Manson and Gary Halford

Lewis Research Center
Cleveland, Ohio

NATIONAL AERONAUTICS AND SPACE ADMINISTRATION

A METHOD OF ESTIMATING HIGH TEMPERATURE LOW CYCLE FATIGUE

BEHAVIOR OF MATERIALS

by S. S. Manson and Gary Halford

Lewis Research Center
National Aeronautics and Space Administration
Cleveland, Ohio

ABSTRACT

A method is described whereby static tensile and creep-rupture properties can be used to estimate lower bound, average, and upper bound low cycle fatigue behavior in the creep range. The method is based primarily on the method of universal slopes previously developed for estimating room temperature fatigue behavior, and in part on a highly simplified creep-rupture - fatigue analysis. Reasonable agreement is obtained when the estimates are compared with total strain range-life data for numerous engineering alloys. Included in the study are coated and uncoated nickel-base alloys, a cobalt-base alloy, low and high alloy steels, and stainless steels tested under laboratory conditions over a wide range of temperatures and cyclic rates.

INTRODUCTION

Low cycle strain-controlled fatigue is now recognized as an important failure mode in some components of gas turbines, nuclear reactors and other high-temperature systems. The amount of readily available data on laboratory samples is still quite limited, and hence, estimates of the performance of specific materials of engineering interest are very useful in the early stages of design and materials selection.

Several studies have recently been described that provide estimates of the low cycle fatigue characteristics of materials at elevated temperatures (e.g., refs. 1 and 2). The simplified approach of reference 2 is based on the method of universal slopes that had previously been developed for estimating room temperature fatigue behavior of small laboratory samples (refs. 3 and 4). Since the universal slopes equation contains constants obtainable from only simple tensile test properties - elastic modulus, ultimate tensile strength, and percent reduction of area - a first attempt was to apply this equation using the tensile properties at the high temperature of interest. For the few cases in which a direct comparison was possible, it was found that the lives predicted in this way were substantially higher than were realized experimentally. The discrepancy was especially apparent when the high temperature fatigue cracks were intercrystalline. Several procedures were then examined for modifying the equation for high temperature use, based largely on the concept that intercrystalline cracks, occurring as a "creep effect", serve as fatigue nuclei. Some of the procedures involved separating the crack initiation and propagation stages of fatigue and applying a different cycle reduction factor to each. However, the procedure designated as the "10% Rule" avoided the difficulties involved in the separation of the two stages by applying a single factor to the entire life rather than different factors to each stage. Only a few materials were evaluated, however, limiting the generality of conclusions drawn in that report (ref. 2).

This report represents a continuation of the study to provide simple modifications to the universal slopes equation for estimating high temperature strain-controlled low cycle fatigue behavior of laboratory size samples. By examining the behavior of numerous high temperature engineering materials tested over wide ranges of conditions, more meaningful conclusions are derived regarding the validity of the universal slopes equation and modifications that can be applied to it to improve its accuracy. It is believed that the conclusions drawn from analyses of the many materials and test variables examined should provide valuable guidelines for the estimation of the high temperature fatigue behavior of new materials as well. The results of our study, and the simplified rules derived therefrom, are described in the following sections.

METHOD

The method that has evolved from the study is based on observations made in attempting to apply the universal slopes equation, and modifications thereto, to numerous sets of high temperature fatigue data. On the basis of these observations several rules of estimation are established that are believed to be useful. The method is as follows:

For selected values of total strain range, $\Delta\epsilon_t$, determine cyclic life values, N_f, according to the universal slopes equation (ref. 3)

$$\Delta\epsilon_t = \frac{3.5\ \sigma_u}{E}\ N_f^{-0.12} + D^{0.6}N_f^{-0.6} \tag{1}$$

where

σ_u = ultimate tensile strength

E = modulus of elasticity

D = ductility = $\ln\left(\dfrac{100}{100 - RA}\right)$ where RA is the percent reduction of

      area as measured in the conventional tensile test

The properties σ_u, E, and D are determined at the high temperature of

interest at moderate strain rates normally employed in conventional

tensile testing (say, arbitrarily, within a factor of 10 of that specified

by ASTM Standards). For the most part, estimates of cyclic life can be

based on certain percentages of N_f as determined from equation (1).

    However, extreme cases involving low frequencies and relatively high

temperatures occasionally arise when the failures are primarily time de-

pendent and it becomes necessary to make an additional estimation of life,

N_f', according to

$$N_f' = \frac{N_f}{1 + \dfrac{k}{AF}\left(N_f\right)^{\frac{m+0.12}{m}}} \tag{2}$$

    Equation (2) represents a highly simplied attempt to account for the

creep-rupture damage associated with the application of stress at high

temperature. It should be considered as an interim approach owing to the

assumptions made in deriving the equation. These assumptions and their

limitations are discussed in the Appendix. In this equation

k = effective fraction of each cycle for which the material may be con-
sidered to be subjected to the maximum stress. For reasons given
in the Appendix, k is taken to be 0.3 in this report.

F = frequency of stress application, cycles per minute (0.0167 Hz) used
in this report.

A = coefficient characterising a time intercept of the creep-rupture
curve of the material at test temperature. The curve of stress,
σ_r, against rupture time, t_r, is linearized on logarithmic
coordinates, and represented by the equation

$\sigma_r = 1.75\sigma_u\left(\dfrac{t_r}{A}\right)^m$, so that A is the time intercept at an ex-
trapolated value of $\sigma_r = 1.75\ \sigma_u$.

m = slope of creep-rupture line (negative value).

N_f = life calculated from equation (1).

Equation (2) is applicable only if $N_f' < 10\%\ N_f$ and if $N_f' < 10^5$
cycles. Figure 1 provides a simple criterion for determining whether the
use of equation (2) is necessary. If the point representing the coordinates
m and AF which apply to the test conditions of the material lies above
the curve and above the lowest coordinates shown, N_f' is computed according
to equation (2); if below the curve, N_f' need not be computed.

By use of equations (1) and (2), estimates of elevated temperature
low cycle fatigue behavior can be made as follows:

1. As an estimate of the lower bound of life use either 10% N_f or
N_f', whichever is the lower.

2. As an estimate of average life use two times the lower bound life.

3. As an estimate of upper bound of life use 10 times the lower bound life.

The application of this method to numerous sets of fatigue data will be discussed in a later section.

SOURCES OF DATA FOR ANALYSIS

To evaluate the method, high temperature fatigue data have been culled from many sources (refs. 5 to 14) such as existing literature, tests conducted in the authors' laboratory and previously unpublished contributions generously submitted by various investigators. Forty sets of data are included in the analysis comprising 354 data points in the life range from 10 to 10^5 cycles at temperatures above 1000° F (811° K). Table I presents the alloys, test conditions, and the pertinent tensile and creep-rupture properties at the fatigue test temperature. Usually the tensile properties were cited in the reference source. In the cases where they were not supplied, handbook or other reference source data were used as noted in the table. The tensile properties are presumed to have been obtained from reasonably standard tests, since in some cases the authors did not cite complete information.

The materials include low and high alloy steels, stainless steels, a cobalt-base alloy, and various nickel-base alloys both in the coated and uncoated condition. Ultimate tensile strengths ranged from 16 to 182 ksi (1.1×10^8 to 12.5×10^8 N/m^2), and reductions of area from 3 to 94 percent. All tests were conducted in uncontrolled air environments at homologous temperatures (ratio of test temperature to melting point, both in degrees

absolute) ranging from 0.48 to 0.88. Test frequencies ranged from 0.017
to 50 cycles per minute (0.00028 to 0.83 Hz), with some tests involving
dwell times at maximum strain of as long as 3 hours (10,800 s).

In most cases the fatigue tests were conducted in axial push-pull,
controlling either the longitudinal or diametral total strain range.
These tests are thus very similar to those reported in reference 3 on
which the method of universal slopes was based. In only two cases, the
Nimonic alloys investigated by Forrest and Armstrong (ref. 11) and the
Cr-Mo-V steel reported by Coles and Skinner (ref. 6), were the tests
conducted in plane bending - although still strain-controlled.

ANALYSIS OF DATA

The low cycle fatigue data are plotted in figures 2(a) to (f) as
total strain range versus cycles to failure on logarithmic coordinates.
Symbols representing the data are left open if the mode of cracking was
not identified in the reference source; shaded if the cracking was
definitely identified as transcrystalline; or an X is enclosed in the
data symbols if the mode of cracking was definitely identified as inter-
crystalline. Also shown in each figure is a set of curves representing
estimates made by the proposed method. The lowest curve shown with each
set of data is the estimate of the lower bound using the rule associated
with 10% N_f or N_f'; the middle curve is the estimate of the average
behavior; and the upper curve is the estimate of the upper bound. The
dashed sections of the curves (figs. 2(d) and (e) only) indicate that
equation (2) was used in making the estimates, whereas the continuous
curves represent estimates based on equation (1).

Examination of figures 2(a) to (f) shows that a reasonably good estimate of the experimental results can be achieved by the method outlined. Since the rules were, to some extent, derived from examination of the data in these figures, some agreement is inherent. However, recognizing that only a limited number of easily determined tensile and creep-rupture properties are required in making the estimates, the agreement with experimental data is gratifying. Hence, a degree of confidence is established in the possibility of applying these estimates to other materials or test conditions.

It is also seen in figures 2(a) to (f) that, for a given temperature and strain range, life decreases as the cycling frequency is decreased (figs. 2(b), (d), and (e)), and that the lower frequencies seem to promote intercrystalline cracking. When intercrystalline cracking occurs, the lives lie closer to the lower bound than when the failures are definitely transcrystalline. In the relatively few cases for which the creep-rupture calculation (eq. (2)) was applicable, the failures were always intercrystalline (figs. 2(d) and (e)). However, occasional low lives were observed where intercrystalline cracking was dominant, even though the creep-rupture properties did not indicate a need for the N_f' calculation (figs. 2(a), (d), and (f)). Whether these results are due to inadequate creep-rupture information (usually, handbook values were used to estimate creep-rupture behavior), or whether they are due to inadequacies of the method requires further study. Some of the limitations of the method are discussed later in the report.

Although figures 2(a) to (f) provide a visual picture of the relative validity of the method when applied to individual materials, a more complete over-all evaluation of the method can be made with the aid of figure 3. This figure shows a direct comparison of the observed with the estimated fatigue lives for all of the materials collectively. The abscissa is the estimated average life, determined according to item (2) of the section describing the METHOD. On the ordinate is plotted the observed life. The symbols represent the experimental data points, using the same conventions as in figures 2(a) to (f). Perfect agreement between experimental results and estimates computed from tensile and creep-rupture properties would be obtained if all the data points coincided with the 45° line AB. The lower line CD represents the estimated lower bound on life, according to item (1), and the upper line EF is the estimated upper bound according to item (3).

The table in figure 3 provides an analysis of the degree to which the estimated average lives and upper and lower bounds agree with the experimental data. For 97% of the data points, the line EF serves as an upper bound, and of the remaining 3%, all but two of the points lie within a factor of 1.5 greater than the upper bound. The line CD serves as a lower bound for 81% of the data, and the distribution of the remaining 19% is tabulated in the figure as a function of the life factor below the lower bound. Since most of the points falling below CD are within a life factor of 2 below it, a more conservative estimate of the lower bound is given by C'D' (5% N_f or 1/2 N_f', whichever is lower). This more conservative lower bound embraces 95% of the data. The table also lists

the distribution of the data points from the average life line AB by life factors of 2, 5, and 10. Here the life factor refers to either an over- or under-estimation of life. This is the same as was done in reference 3 for evaluating the applicability of the method of universal slopes to the estimation of the average room temperature fatigue behavior of 29 materials. The table shows that the validity of the high temperature method for estimating average life behavior is comparable to that of the method of universal slopes when applied to room temperature results.

DISCUSSION

The method as described for estimating elevated temperature low cycle fatigue behavior is highly simplified, and does not consider many of the complicating factors that influence the low cycle fatigue characteristics in the creep range. To obtain greater accuracy more attention must be paid to the details of the fatigue and creep processes and the factors that affect the life. The importance of refinements and the best procedures are not yet clear; however, a few possible approaches may be outlined as a guide for future study.

One approach might be to retain the simplicity of the universal slopes method, but to take cognizance of the fact that the tensile properties that enter into the equation depend not only on temperature but on strain rate, hold-times, and environment as well. Thus, if the appropriate tensile properties could be determined, the form of the equation would be retained, and only the constants would be altered. This is similar to the approach adopted by Coffin (ref. 1) for a strain-aging material in which strain rate was introduced as a primary consideration. Such an

approach requires, however, the generation of additional experimental data.

Alternatively, it may be useful to redefine the terms that enter into the equations. For example, it may be useful to determine ductility in terms of the strain which causes surface cracking rather than rupture, as suggested by Wells and Sullivan (ref. 12), and to replace tensile strength by some creep-rupture strength (e.g., the stress to cause rupture in a specified time). Such an approach, however, will require extensive and accurate data before the necessary correlations can be made and applied with confidence to new materials.

Another possibility is to take into account some refinements associated with the fatigue process which are of special importance at high temperature. For example, in reference 2, we considered the relative importance of crack initiation and propagation on life at high temperature, and in particular how intercrystalline cracking might influence each of these factors. The discussion was highly speculative owing to the limited data on which to base suitable judgement and make reasonable assumptions. Further pursuit of this approach could be rewarding. Again, additional information will be required before suitable refinements of this type can be applied with confidence.

Finally, procedures for incorporating creep-rupture damage together with fatigue damage as discussed by Taira (ref. 15) or as outlined in the Appendix could be extended further to make them more quantitative. It would be necessary to establish the significance of stress reversal, to determine more accurately how to treat the continuously changing stress, and to establish how to combine creep and fatigue into an appropriate cumulative damage law.

Until such time as more accurate and detailed procedures become available, the method presented in this paper offers an extremely simple way of estimating elevated temperature low cycle fatigue behavior of small laboratory samples from easily attainable tensile test and creep-rupture data. At very high temperatures, low cycling frequencies, or when the creep-rupture curve of stress versus rupture time is relatively steep (log-log slope steeper than -0.12), an additional calculation should be made to obtain a closer estimate of the lower bound of fatigue life. This calculation represents a highly simplified computation of the damage produced by creep-rupture effects.

Although we have demonstrated the degree of confidence that might be expected in our estimations of average lives and upper and lower bounds, care must be exercised in applying the rules given when an application involves extreme test conditions well beyond the range included in this study. For example, the proposed method cannot be expected to apply when continuous strain cycling is interrupted by excessively long hold times spent at a fixed strain where creep-relaxation can occur. However, by extending the general approach given in the Appendix, it may be possible to assess the creep damage induced under such circumstances. In the final analysis, the most appropriate fatigue information is that generated under conditions that simulate as closely as possible those that will be encountered in an actual application. The interpretation of even conventional laboratory fatigue data in terms of service performance provides many difficulties. Hence, even more so can we expect estimates based on tensile

and creep-rupture properties to have their limitations. If these limitations are borne in mind, however, the estimates can be very useful.

CONCLUSIONS

The method of universal slopes, developed for estimating the low cycle fatigue behavior of materials at room temperature from static tensile properties alone, has been extended for application to materials in the creep range. In most instances, the estimates of life are based on certain percentages of the life as computed from the method of universal slopes. As proposed, the method permits the estimation of a reasonable lower bound, average value, and upper bound on fatigue life of strain-controlled laboratory size samples. The method has been checked by comparing the estimates with elevated temperature strain-controlled laboratory fatigue data on numerous materials obtained from various sources. Without excluding data scatter arising from the diverse testing techniques of different laboratories, the results obtained still indicate that the estimates at high temperature can be made with about the same degree of confidence as that obtainable at room temperature with the method of universal slopes.

APPENDIX - CREEP-RUPTURE EFFECT

Some of the damaging effect of exposure to high stress at elevated temperature is inherently accounted for by using 10% N_f as a lower bound. Cases arise, however, when the creep-rupture curve is quite steep (log-log slope steeper than -0.12), the temperature is very high, and the frequency is very low. Under these circumstances more creep damage is done than this rule can account for. In such cases it is necessary to examine the damaging effect more closely. Although a rigorous treatment is beyond the scope of this paper, an elementary approach is suggested on an interim basis until better assumptions can be established by critical experiments.

An important factor to be considered is the magnitude of the stress level that develops during strain cycling. Although estimates must suffice in the present analysis, direct measurement of this stress would, of course, provide a better indication of the damage done. As a first approach, we resort to the method of universal slopes for an estimate of the stress amplitude. If the life were N_f (in the absence of a creep-rupture effect), the stress amplitude, σ_a, can be estimated (ref. 4, Chapter 4), by

$$\sigma_a = \frac{\Delta \epsilon_e E}{2} = \frac{3.5\ \sigma_u}{2}\ N_f^{-0.12} = 1.75\ \sigma_u N_f^{-0.12}$$

It has been our experience that this estimate of the stress amplitude may possibly be a source of considerable error (errors of the order of $\pm$ 20% are not uncommon). Further complications arise in the consideration of how to apportion the damaging effects of tensile and compressive

stresses during strain cycling. The influence of compression has generally been ignored and damage is considered to be caused only by tensile stresses. Whether this concept is realistic is unclear, since it is probable that compressive stresses may be detrimental (by causing grain boundary sliding) or even beneficial (as a result of the "healing" effect of reversed strain). Definitive experiments are necessary to clarify these opposing effects. Another uncertainty arises due to the unknown shape of the stress-time wave form. Ideally, both the shape of the wave form and the slope of the creep-rupture curve must be known to determine the effective fraction of each cycle, k, for which the material may be considered to be subjected to the maximum stress.

For the elementary treatment given here, partial allowance is made for the various uncertainties described by choosing an appropriate value of k that results in fatigue life estimates having quantitative agreement with the available data. Although the best results could be obtained by selecting different values of k for each set of data, a single representative value of 0.3 was found to be reasonable.

Equation (2) can now be derived in the following manner. If N_f' is the <u>actual</u> number of cycles to failure, and the frequency is F cycles per unit time, the time to failure is N_f'/F, and the effective time for which the maximum stress in the cycle acts is $t' = \dfrac{kN_f'}{F}$. It is assumed that the creep-rupture damage is the ratio of the effective time at maximum stress to the creep-rupture time at this stress. The next step, therefore, is to determine the creep-rupture time, t_r, under a steadily applied tensile stress, σ_r, equal to the fatigue stress

amplitude. The creep-rupture curve is represented by a power law

relation $\sigma_r = 1.75\ \sigma_u\left(\dfrac{t_r}{A}\right)^m$, so that the stress-rupture curve on log-log

coordinates becomes a straight line of slope m and time intercept A

at an extrapolated value of $\sigma_r = 1.75\ \sigma_u$ (see inset, fig. 4). Then,

at a stress $\sigma_r = \sigma_a = 1.75\ \sigma_u N_f^{-0.12}$, the creep-rupture time, t_r,

becomes $A(N_f)^{-\frac{0.12}{m}}$. Hence, the creep-rupture damage is given by

$$\frac{t'}{t_r} = \frac{kN_f'}{AF(N_f)^{-\frac{0.12}{m}}}\ .$$

The damage due to pure fatigue is taken to be the ratio of the

actual number of cycles to failure to the cycles that would have been

sustained in the absence of creep damage, that is N_f'/N_f. Assuming a

linear cumulative damage law wherein creep damage is given by time

ratios, and fatigue damage is given by cycle ratios, then at failure

$$\frac{N_f'}{N_f} + \frac{t'}{t_r} = 1 = \frac{N_f'}{N_f} + \frac{kN_f'}{AF(N_f)^{-\frac{0.12}{m}}}$$

or

$$N_f' = \frac{N_f}{1 + \dfrac{k}{AF}\,(N_f)^{\frac{m+0.12}{m}}} \tag{2}$$

This approach is presumed to have utility only when a large creep-

rupture effect is anticipated and the 10% N_f rule is inadequate as a

lower bound; that is, when $N_f' < 10\%\ N_f$. In this region of interest,

failure is primarily time dependent and the fatigue damage is nearly

negligible. Since we have restricted ourselves to observed lives of less than 10^5 cycles, the creep-rupture effect need be considered only when $N_f' < 10\% \ N_f < 10^5$. Hence, if equation (2) indicates that $N_f' > 10\% \ N_f$ for values of $N_f' > 10^5$, further use of equation (2) is not called for. This criterion has been used to construct the curve shown in figure 1 for $k = 0.3$.

An illustration of the estimation procedure for incorporating the creep-rupture effect is shown in figure 4 for Nimonic 90 at 1600° F (1143° K) and $F = 0.1$ cpm (0.0017 Hz) (ref. 11). The inset creep-rupture curve shows that $m = -0.24$ and $A = 2.5$ min. (150s); hence, for $F = 0.1$ cpm (0.0017 Hz) and $k = 0.3$, the point P is determined as shown in figure 1. Since this point lies above the curve, the computation of N_f' from equation (2) is made. The estimate of the lower bound is shown in figure 4 as CDH. In the region CD, 10% N_f (where N_f is determined from curve AB - the method of universal slopes, equation (1)) gives a lower life than N_f' and hence, CD is used instead of GD. At high lives, DH provides a lower life than 10% N_f, thus DH is used instead of DE. Although not shown in figure 4, the average life estimation and the upper bound would be determined by multiplying the lower bound lives by factors of 2 and 10 respectively. These curves would then be the same as those already shown in figure 2(d) for this material and test condition.

REFERENCES

1. L. F. Coffin, Jr., "Proceedings of the First International Conference on Fracture" (Sendai, 1965), 3, Paper No. DI-119. 1966: Japan (Japanese Society for Strength and Fracture of Materials).

2. S. S. Manson, Int. J. Fracture Mechanics, 1966, 2, (1), 327.

3. S. S. Manson, Exp. Mechs., 1965, 5, (7), 193.

4. S. S. Manson, "Thermal Stress and Low-Cycle Fatigue". 1966: New York (McGraw-Hill).

5. V. H. Thevenow, Allison Division of General Motors, Materials Laboratory Report No. MSM 6-13, 1966.

6. A. Coles and D. Skinner, Roy. Aeronautical Soc. J., 1965, 69, (649), 53.

7. W. F. Anderson and C. R. Waldron, Atomics International, North American Aviation Report No. NAA-SR-4051, 1959.

8. Anon., General Electric Progress Report No. 58, Part A, GEMP-58A, 1966.

9. T. Slot, General Electric Report No. GE-TM66-6-11, 1966.

10. E. E. Baldwin, G. J. Sokol, and L. F. Coffin, Jr., Proc. Amer. Soc. Test. Mat., 1957, 57, 567.

11. P. G. Forrest and K. B. Armstrong, "Joint Int. Conf. on Creep" (New York-London, 1963), Paper No. 1. 1963: London (Institution of Mechanical Engineers). See also: P. G. Forrest and K. B. Armstrong, J. Inst. Metals, 1966, 94, (6), 204.

12. C. H. Wells and C. P. Sullivan, Trans. Amer. Soc. Metals, 1965, 58, (3), 391.

13. R. W. Swindeman, "Joint Int. Conf. on Creep" (New York-London, 1963), Paper No. 32. <u>1963</u>: London (Institution of Mechanical Engineers).

14. Anon., Data courtesy of Pratt and Whitney Aircraft, Division of United Aircraft Corporation, East Hartford, Connecticut.

15. S. Taira, "Creep in Structures", p. 96, <u>1962</u>: New York (Academic Press).

TABLE I. - ALLOYS, TEST CONDITIONS, AND PERTINENT PROPERTIES

Alloy designation	Test temperature		Test frequency, F		RA, percent	Tensile strength, σ_u		Elastic modulus, E		Creep-rupture			Reference
	°F	°K	cpm	Hz		ksi	10^8 N/m^2	10^3 ksi	10^{11} N/m^2	Slope	Intercept, A		
										-m	min	s	
A-286-CR 34%	1000	811	5-50	0.083 - 0.83	31.	182.	12.5	26.8	1.85	<0.12	-----	------	*
	1200	923	5-50	.083 - 0.83	38.	167.	11.5	23.1	1.59	<.12	-----	------	
A-286-Aged	1200	923	5-50	0.083 - 0.83	18.	115.	7.93	23.0	1.59	<0.12	-----	------	
A-286	1400	1033	20	0.33	57.6	75.	5.2	19.0	1.31	0.20	1.3	72.	(5)
Inco 901	1400	1033	20	0.33	16.1	104.	7.17	20.8	1.43	0.135	0.028	0.17	
D-979	1260	956	5-50	0.083 - 0.83	42.	179.	12.3	22.0	1.52	<0.12	-----	------	*
Cr-Mo-V Steel	1050	838	1, 10	0.017, 0.17	70.	69.5	4.79	24.**	1.65	<0.12	-----	------	(6)
L-605	1000	811	5-50	0.083 - 0.83	48.2	106.	7.31	27.	1.9	<0.12	-----	------	*
	1200	923	5-50	.083 - 0.83	47.1	95.4	6.58	25.	1.7	<.12	-----	------	
304 Stainless steel	1000	811	10	0.17	67.3	55.5	3.83	23.**	1.6	<0.12	-----	------	(7)
	1200	923	3-18	.05 - 0.30	58.**	41.**	2.8	22.**	1.5	.18	15.0	900.	(8)
	1500	1089	3-27	.05 - 0.45	42.**	20.**	1.4	19.**	1.3	.18	.3	18.	(9)
347 Stainless steel	1110	873	----------	----------------	67.7	55.**	3.8	22.**	1.5	<0.12	-----	------	(10)
Nimonic 75	1200	923	10	0.17	29.5	81.5	5.62	20.3**	1.40	------	-----	------	(11)
	1380	1023	10	.17	42.0	53.1	3.66	15.4**	1.06	------	-----	------	
	1600	1143	10	.17	62.5	28.0	1.94	12.2**	.84	------	-----	------	
	1800	1253	10	.17	66.0	16.2	1.12	9.7**	.67	------	-----	------	
Nimonic 90	1200	923	10	0.17	24.5	144.	9.93	26.5**	1.83	<0.12	-----	------	
	1380	1023	0.1, 10	.0017, 0.17	12.0	119.	8.20	25.**	1.7	.135	0.16	9.6	
	1600	1143	0.1, 10	.0017, 0.17	14.0	76.	5.2	23.**	1.6	.24	2.5	150.	
	1800	1253	0.1, 10	.0017, 0.17	94.0	16.	1.1	21.**	1.45	.25	4.0	240.	
Nimonic 105	1200	923	10	0.17	13.7	142.	9.79	25.**	1.7	<0.12	-----	------	
	1380	1023	10	.17	18.0	151.	10.4	23.5**	1.62	<.12	-----	------	
	1600	1143	10	.17	32.5	99.5	6.86	22.**	1.5	.16	0.08	4.9	
	1800	1253	10	.17	68.0	39.2	2.70	19.**	1.3	.28	3.7	222.	
Udimet 700	1400	1033	1-2	0.017 - 0.033	31.	155.	10.7	23.	1.6	<0.12	-----	------	(12)
Astroloy	1400	1033	20	0.30	29.6	141.	9.72	23.	1.6	<0.12	-----	------	(5)
Inconel	1500	1089	0.017, 0.1	0.00028, 0.0017	63.3	25.	1.7	18.	1.2	0.15	1.0	60.	(13)
IN 100 (PWA 47 Coat)	1000	811	6	0.10	9.3	121.	8.34	27.1	1.87	<0.12	-----	------	(14)
	1700	1200	6	.10	11.	96.	6.6	22.7	1.57	.17	0.11	6.6	
	2000	1367	6	.10	10.3	26.8	1.85	19.3	1.33	.22	1.3	78.	
MAR M 200 (PWA 47 Coat)	1300	978	6	0.10	5.	120.	8.27	26.5	1.83	<0.12	-----	------	
	1700	1200	6	.10	4.	77.	5.3	23.7	1.63	<.12	-----	------	
B 1900 (PWA 47 Coat)	1300	978	6	0.10	5.	145.	10.0	25.5	1.76	<0.12	-----	------	
	1700	1200	6	.10	3.	95.	6.5	23.0	1.59	.17	0.75	45.	
	2000	1367	6	.10	9.	35.	2.4	20.5	1.41	.26	7.5	440.	

*NASA data - E. R. Roberts.

**Approximate handbook values.

Note: If point is above curve, N_f' should be
calculated from Equation (2). If point
is below curve, or below the lowest
coordinates shown, N_f' need not be
calculated.

⊗ P (Nimonic 90 - 1600° F (1143° K) -
0.1 cpm (0.0017 Hz))

Equation (2) for k = 0.3 and $N_f' = 10^5 = 10$ percent N_f

Slope of creep-rupture curve, −m

Product of creep-rupture coefficient and frequency, AF
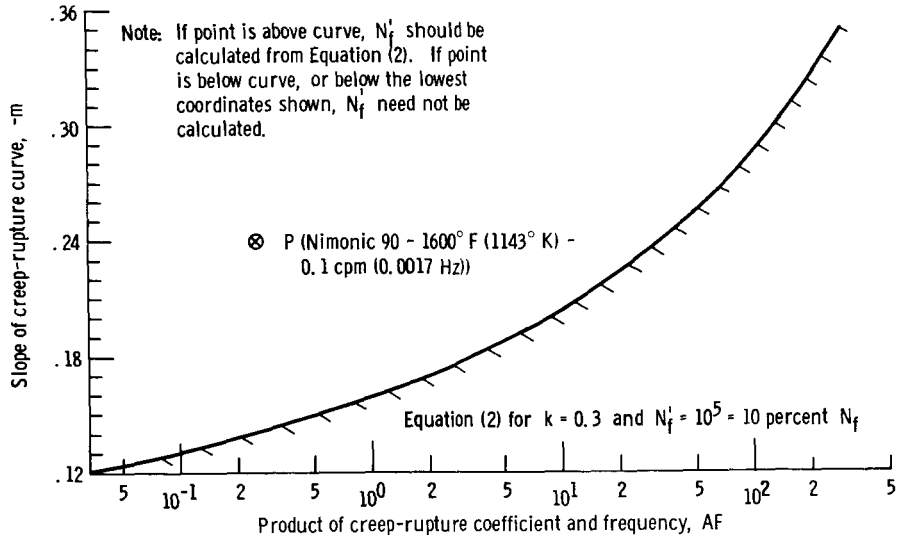
Figure 1. − Criterion for establishing whether equation (2) should be used in estimating high
temperature low cycle fatigue behavior.

5-50 cpm (0.083-0.83 Hz)

5-50 cpm (0.083-0.83 Hz)

Roberts (NASA)
A-286 CR 34 percent
1000° F (811° K)

Roberts (NASA)
A-286 CR 34 percent
1200° F (923° K)

Roberts (NASA)
A-286 Aged
1200° F (923° K)

Thevenow (5)
A-286
1400° F (1033° K)

5-50 cpm (0.083-0.83 Hz)

20 cpm (0.33 Hz)

5-50 cpm (0.083-0.83 Hz)

Thevenow (5)
Inco 901
1400° F (1033° K)

Roberts (NASA)
D-979
1260° F (956° K)·

20 cpm (0.33 Hz)

Total strain range, $\Delta \varepsilon_t$

Cycles to failure
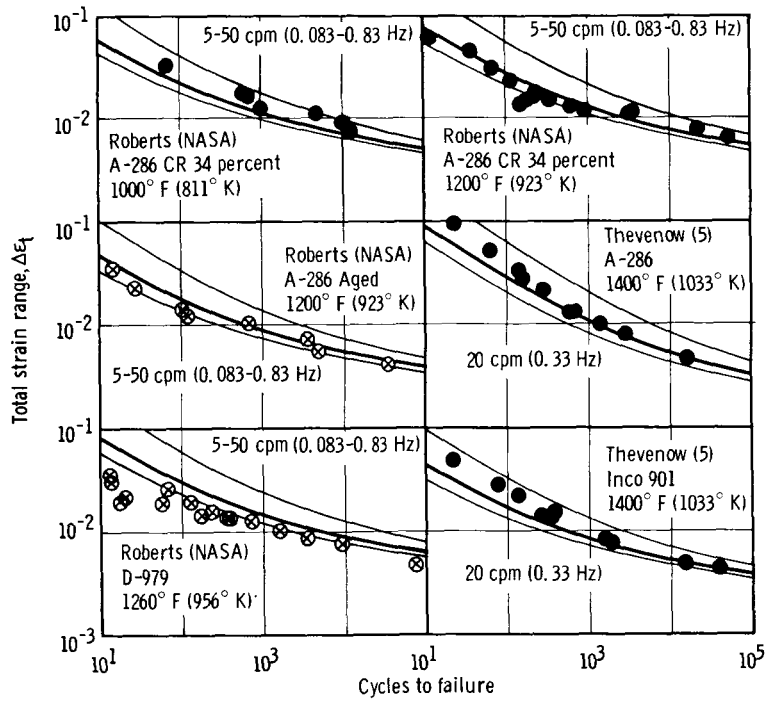
(a) Iron-nickel-chromium-molybdenum alloys.

Open symbols − Unidentified cracking
Shaded symbols − Transcrystalline cracking
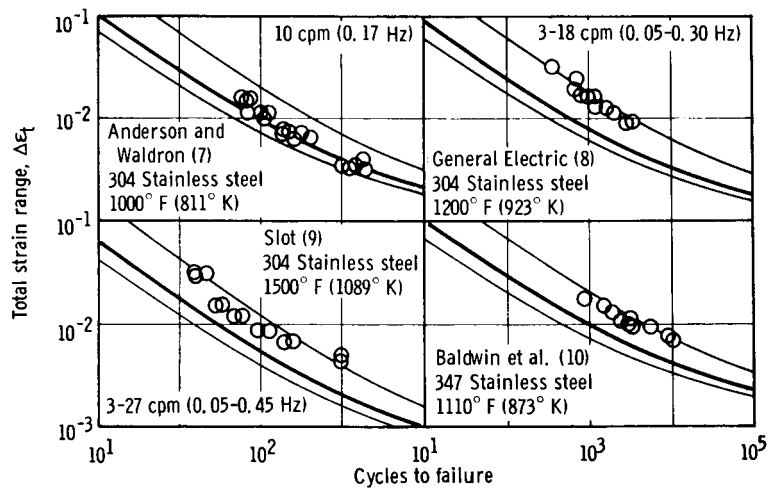X in symbol − Intercrystalline cracking

Based on N_f {
——— Upper bound − − −
——— Average life — — —
——— Lower bound — — —
} Based on N_f' (appears
only in fig. 2(d) and (e))

Figure 2. − Comparison of estimated and observed fatigue behavior.
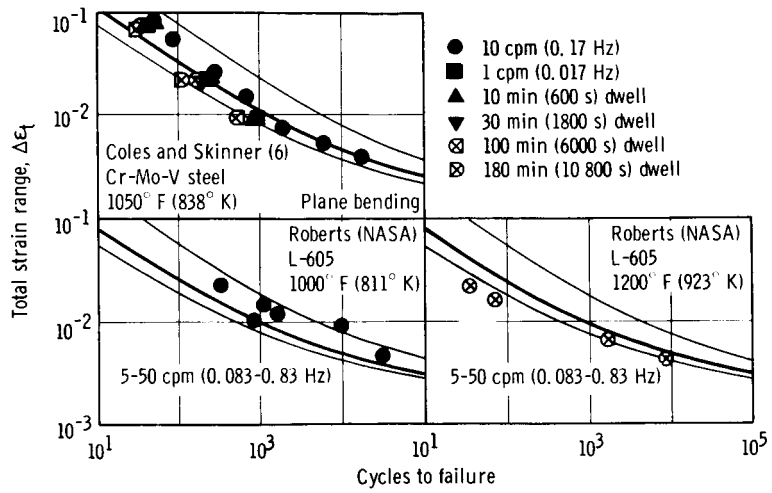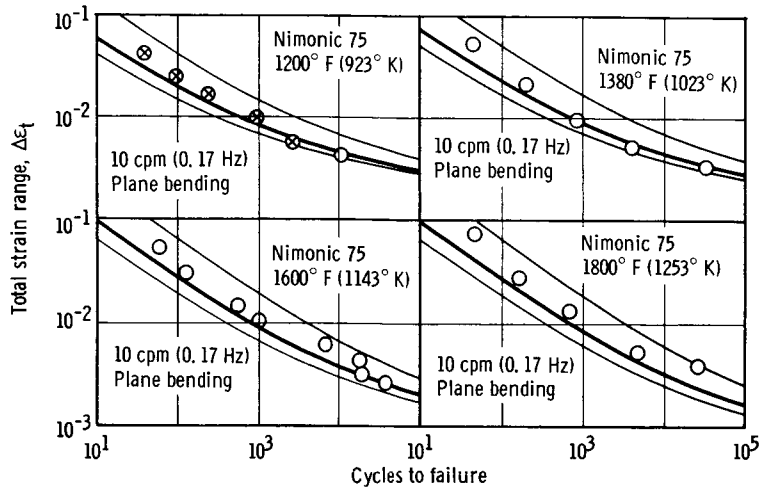
(b) Cr−Mo−V steel and cobalt-base alloy.
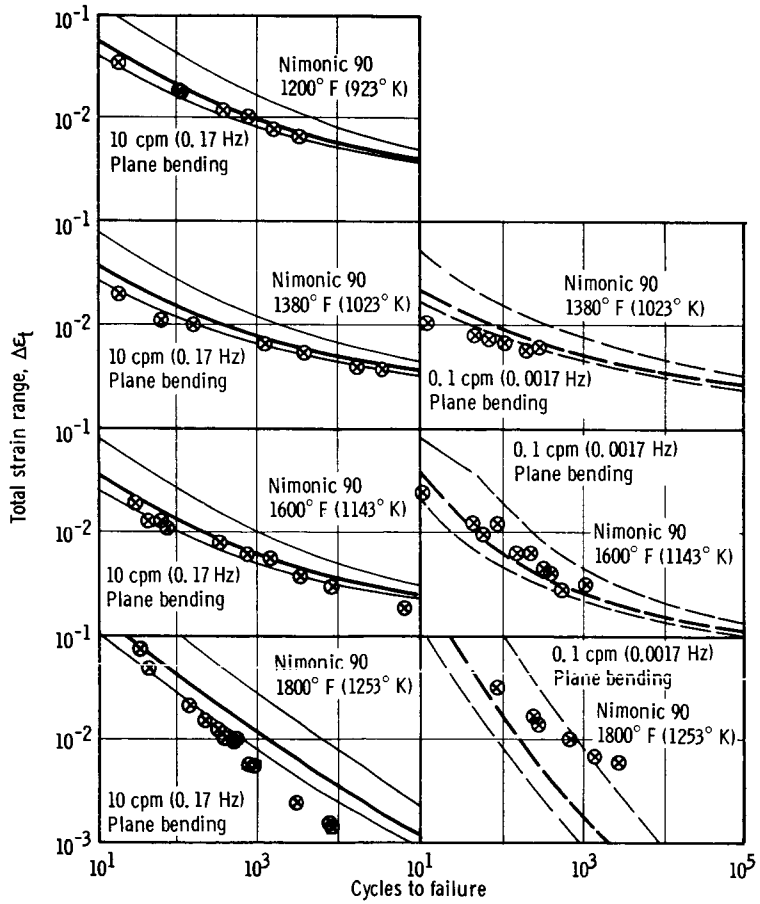
Figure 2. − Continued.
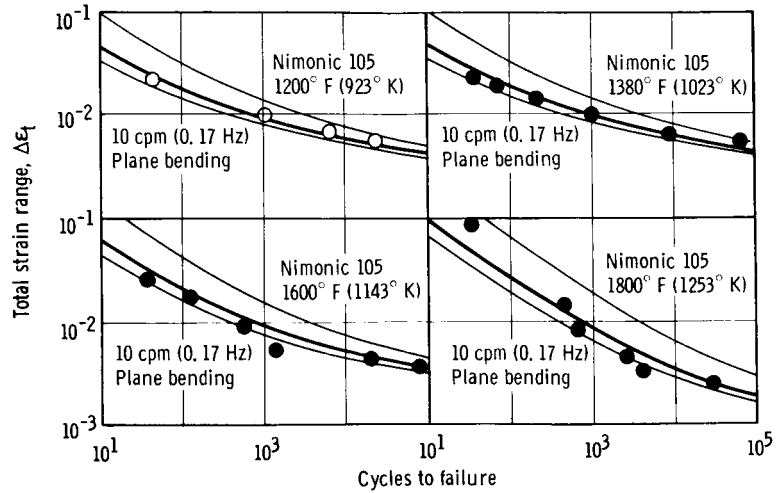

(c) Stainless steels.

Figure 2. − Continued.

(d) Nickel-base alloys – Nimonic series, Forrest and Armstrong (11).
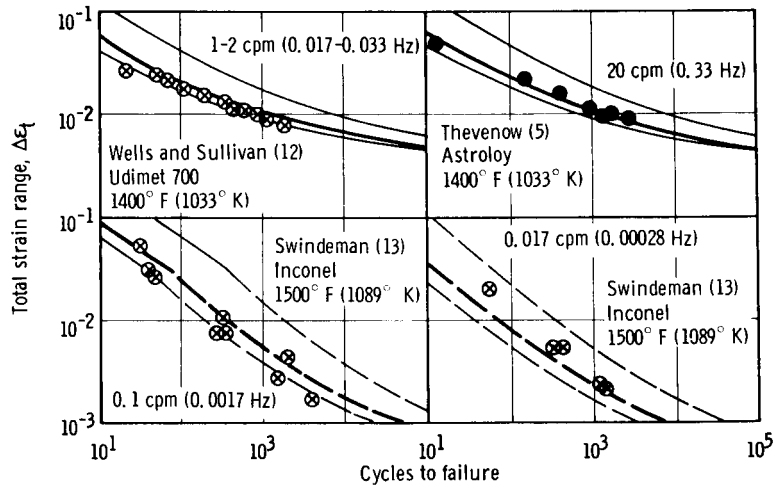
Figure 2. – Continued.

(d) Continued. Nickel-base alloys – Nimonic series, Forrest and Armstrong (11).
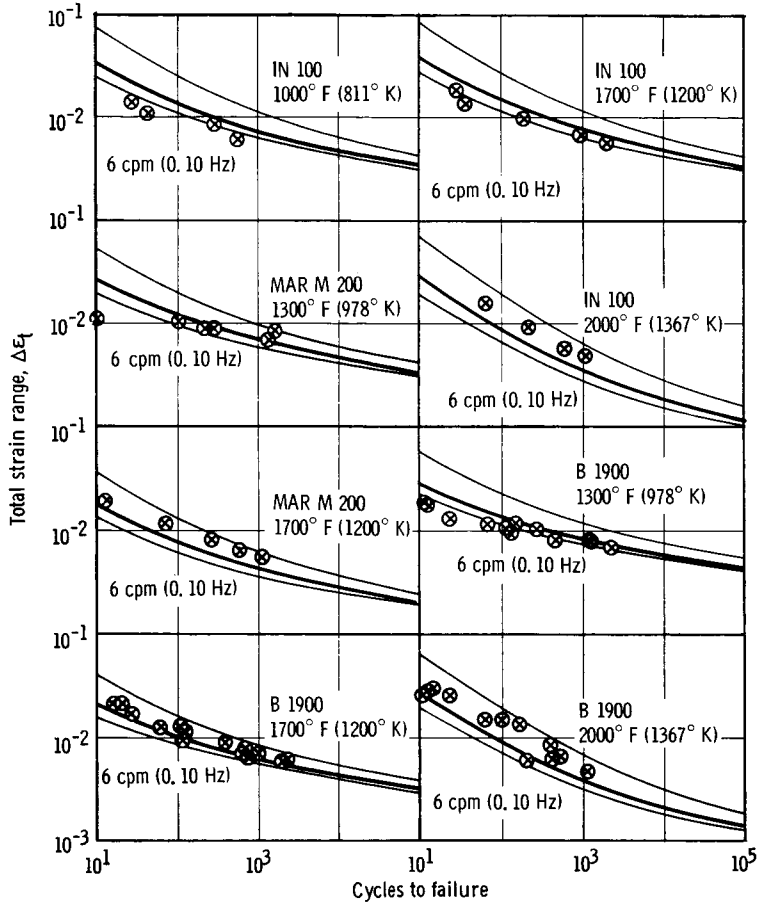
Figure 2. – Continued.

(d) Concluded. Nickel base alloys – Nimonic series, Forrest and Armstrong (11).

Figure 2. – Continued.

(e) Nickel-base alloys.

Figure 2. – Continued.

(f) Coated (PWA 47) nickel-base alloys, Pratt & Whitney (14).

Figure 2. – Concluded.

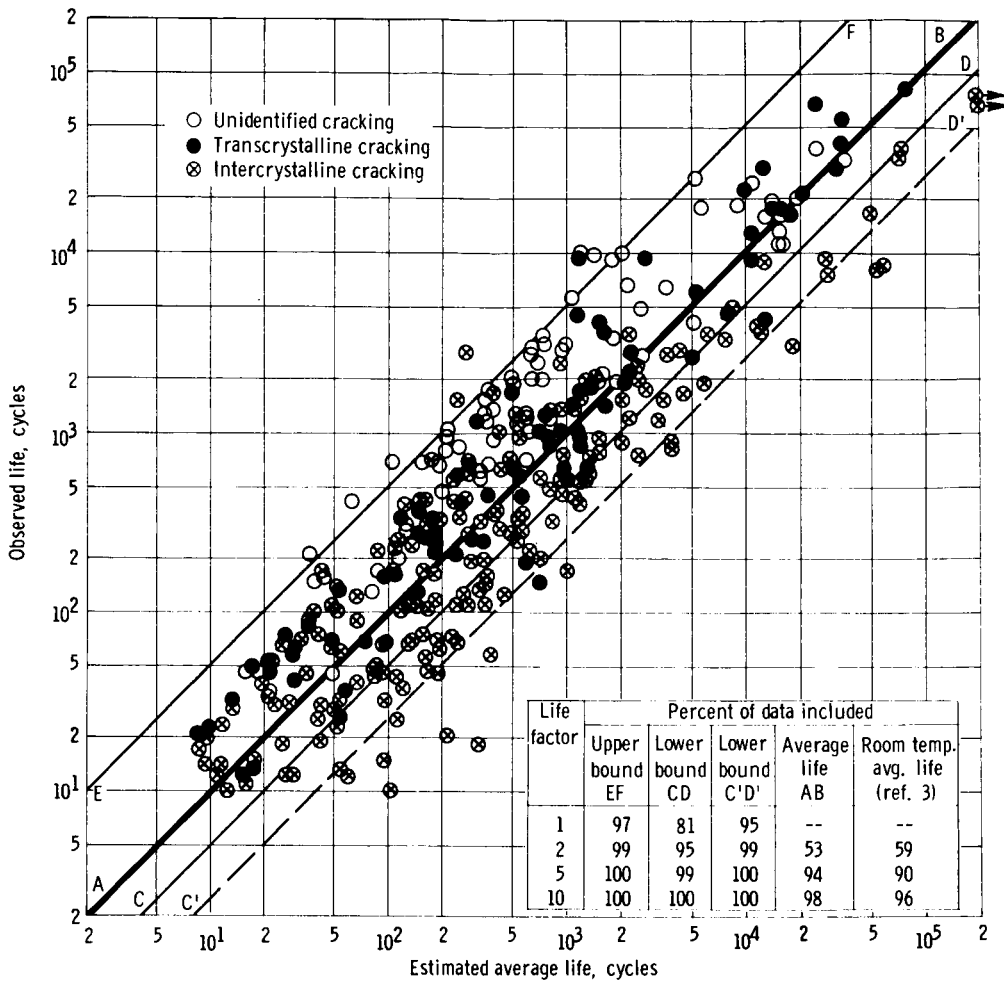| Life factor	Percent of data included				
	Upper bound EF	Lower bound CD	Lower bound C'D'	Average life AB	Room temp. avg. life (ref. 3)
1	97	81	95	--	--
2	99	95	99	53	59
5	100	99	100	94	90
10	100	100	100	98	96

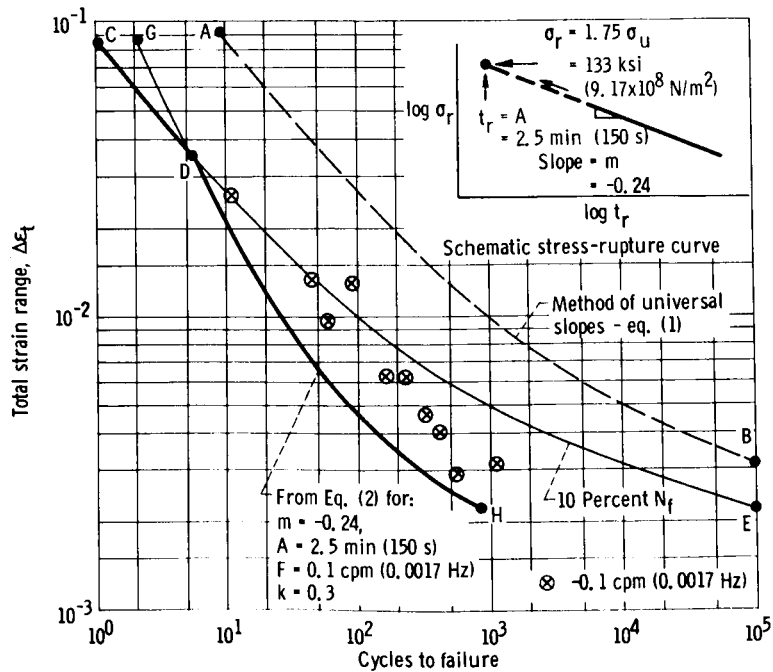Figure 3. – Comparison of observed fatigue life with high temperature method of estimation.

Figure 4. – Creep-rupture effect calculation used to establish lower bound for Nimonic 90 at 1600° F (1143° K) and 0.1 cpm (0.0017 Hz).